

GAMMA-RAY LUMINOSITY AND DEATH LINES OF PULSARS WITH OUTER GAPS

L. ZHANG,^{1,2} K. S. CHENG,³ Z. J. JIANG,² AND P. LEUNG³

Received 2003 July 14; accepted 2003 December 4

ABSTRACT

We reexamine the outer-gap size by taking the geometry of the dipole magnetic field into account. Furthermore, we also consider that instead of taking the gap size at half of the light cylinder radius to represent the entire outer gap, it is more appropriate to average the entire outer-gap size over the distance. When these two factors are considered, the derived outer-gap size $f(P, B, \langle r \rangle(\alpha))$ is a function not only of the period P and magnetic field B of the neutron star but also of the average radial distance to the neutron star, $\langle r \rangle$, which depends on the magnetic inclination angle α . We use this new outer-gap model to study the γ -ray luminosity of pulsars, which is given by $L_\gamma = f^3(P, B, \langle r \rangle(\alpha))L_{\text{sd}}$, where L_{sd} is the pulsar spin-down power, and to study the death lines of γ -ray emission of the pulsars. Our model can predict the γ -ray luminosity of an individual pulsar if its P , B , and α are known. Since different pulsars have different α , this explains why some γ -ray pulsars have very similar P and B but very different γ -ray luminosities. In determining the death line of γ -ray pulsars, we have used a new criterion based on a concrete physical property, i.e., that the fractional size of the outer gap at the null-charge surface for a given pulsar cannot be larger than unity. In an estimate of the fractional size of the outer gap, two possible X-ray fields are considered: (1) X-rays produced by neutron star cooling and polar-cap heating, and (2) X-rays produced by the bombardment of relativistic particles from the outer gap onto the stellar surface (the outer gap is called a “self-sustained outer gap”). Since it is very difficult to measure α in general, we use a Monte Carlo method to simulate the properties of γ -ray pulsars in our Galaxy. We find that this new outer-gap model predicts many more weak γ -ray pulsars, which have a typical age between 0.3 and 3 Myr, than does the old model. For all simulated γ -ray pulsars with self-sustained outer gaps, the γ -ray luminosity L_γ satisfies $L_\gamma \propto L_{\text{sd}}^\delta$, where the value of δ depends on the sensitivity of the γ -ray detector. For EGRET, $\delta \sim 0.38$, whereas $\delta \sim 0.46$ for GLAST. For γ -ray pulsars with $L_{\text{sd}} \lesssim L_{\text{sd}}^{\text{crit}}$, $\delta \sim 1$, and $L_{\text{sd}}^{\text{crit}} = 1.5 \times 10^{34} P^{1/3}$ ergs s^{−1} is determined by $f(\langle r \rangle \sim r_L) = 1$. These results are roughly consistent with the observed luminosity of γ -ray pulsars. These predictions are very different from those of the previous outer-gap model, which predicts a very flat relation between L_γ and L_{sd} .

Subject headings: gamma rays: theory — pulsars: general — stars: neutron

1. INTRODUCTION

High-energy emission models for rotation-powered pulsars are generally divided into polar-gap and outer-gap models. In polar-gap models, charged particles are accelerated in charge-depleted zones near the pulsar’s polar cap, and γ -rays are produced through curvature-radiation-induced γ - B pair cascades (e.g., Harding 1981; Daugherty & Harding 1996; Zhang & Harding 2000) or through Compton-induced pair cascades (Dermer & Sturmer 1994). In the outer-gap models, it is generally accepted that a magnetosphere of charge density

$$\rho_0 \approx \frac{\Omega \cdot \mathbf{B}}{2\pi c} \quad (1)$$

surrounds a rotating neutron star with magnetic field \mathbf{B} and angular velocity Ω (Goldreich & Julian 1969). The magnetospheric plasma corotates with the neutron star within the light cylinder, at which the corotating speed equals the velocity of light and the distance from the spin axis is $R_L = c/\Omega$. In the corotating magnetosphere, the electric field along the magnetic field, $E_\parallel = \mathbf{E} \cdot \mathbf{B}/B$, is nearly zero. However, the flow of the plasma along open field lines results in some

plasma void regions (where the charge density is significantly different from ρ_0) in the vicinity of null-charge surfaces, where $\Omega \cdot \mathbf{B} = 0$ (Hollaway 1973). In such charge-deficient regions, which are called “outer gaps,” $E_\parallel \neq 0$ is sustained, electrons and positrons can be accelerated to relativistic energies, and the subsequent high-energy γ -ray emission and photon-photon pair production can maintain the current flow in the magnetosphere (Cheng, Ruderman, & Sutherland 1976; Cheng, Ho, & Ruderman 1986a, 1986b, hereafter CHR I and CHR II; Romani 1996; Zhang & Cheng 1997; Hirotani 2001).

Based on known γ -ray pulsars, the luminosity and conversion efficiency of γ -rays in various models have been studied (e.g., Harding 1981; Dermer & Sturmer 1994; Rudak & Dyks 1998; Yadigaroglu & Romani 1995; Zhang & Cheng 1998). Observations by the *Compton Gamma-Ray Observatory* show that the γ -ray luminosity of rotation-powered pulsars is proportional to square root of the spin-down power (Thompson 2001). Using new polar-gap models (e.g., Zhang & Harding 2000; Harding & Muslimov 2001; Harding, Muslimov, & Zhang 2002), Harding et al. (2002) have studied the death lines of γ -ray pulsars based on the predicted luminosity of $L_\gamma \propto L_{\text{sd}}^\delta$, where $\delta \sim 0.5$ when $L_{\text{sd}} \gtrsim L_{\text{sd}}^{\text{break}}$, $\delta \sim 1$ when $L_{\text{sd}} \lesssim L_{\text{sd}}^{\text{break}}$, and $L_{\text{sd}}^{\text{break}} = 5 \times 10^{33} P^{-1/2}$ ergs s^{−1}.

For a rapidly rotating pulsar, it is believed that its spin-down power L_{sd} is converted into radiation energy. Because the outer gap occupies only a part of the open field line region, the γ -ray luminosity produced in the outer gap is a fraction of the spin-down power. It has been shown that the γ -ray luminosity in the outer gap is proportional to f^3 , i.e., $L_\gamma \approx f^3 L_{\text{sd}}$ (CHR II; Zhang

¹ National Astronomical Observatories/Yunnan Observatory, Chinese Academy of Sciences, P.O. Box 110, Kunming, Yunnan 650011, People’s Republic of China.

² Department of Physics, Yunnan University, Kunming, Yunnan 650011, People’s Republic of China.

³ Department of Physics, University of Hong Kong, Hong Kong, People’s Republic of China.

& Cheng 1997). In previous works, the fractional size of the outer gap depends only on the period and magnetic field for a γ -ray pulsar. For example, the fractional size of the outer gap for Crab-like pulsars is $f \propto B_{12}^{-13/20} P^{33/20}$ (CHR II). In the outer-gap model described by Zhang & Cheng (1997), $f \propto B^{-4/7} P^{26/21}$, the observed γ -ray luminosities for energies greater than 100 MeV from known γ -ray pulsars (except for the Crab pulsar) can be approximately explained (Zhang & Cheng 1998). It should be noted that the model predicts that γ -ray pulsars with the same values of $(B/P)^{0.3}$ will have the same γ -ray luminosities. For example, the ratio of $(B/P)^{0.3}$ for PSR B1055–52 to that for Geminga is ~ 0.9 ; this means that the ratio of the γ -ray luminosities should be ~ 0.9 . However, the observed ratio of the luminosities at energies greater than 100 MeV of these two pulsars is ~ 8 (Kaspi et al. 2000). Briefly, seven known γ -ray pulsars have rather different γ -ray luminosities, even though their spin-down powers and ages are very similar (e.g., Geminga and PSR 1055–52). Their pulse shapes also differ very much. It is clear that there are other intrinsic parameters that control these observed properties (γ -ray luminosity, pulse shape, spectrum, etc.).

In this paper we restudy the γ -ray emission from the outer gaps of rotation-powered pulsars by using a new outer-gap model. We follow the idea of the self-sustained outer gap given by Zhang & Cheng (1997). However, we take the magnetosphere geometry, as well as the average properties of the entire outer gap, into consideration and show that the fractional size of the outer gap is a function of period, magnetic field, and magnetic inclination angle. In fact, the effect of the inclination angle on the γ -ray emission has been considered in other versions of the outer-gap model. For example, Romani & Yadigaroglu (1995) and Yadigaroglu & Romani (1995) took the magnetic inclination angle into account in their outer-gap models, and Hirotani and his colleagues also included the magnetic inclination angle in their calculation of the outer-gap model (e.g., Hirotani 2001; Hirotani & Shibata 2001, 2002; Hirotani, Harding, & Shibata 2003). Differently from the treatment of Romani & Yadigaroglu (1995), who considered it in a less analytic way, we give an explicit expression for the fractional size of the outer gap. In § 2 we describe the revised outer-gap model. We estimate the γ -ray luminosities for rotation-powered pulsars and compare them with the observed data in § 3. In § 4 we derive the death lines of pulsars with outer gaps. Finally, we briefly give our discussion and conclusion.

2. THE OUTER-GAP MODEL

2.1. Magnetospheric Geometry

For an oblique magnetic dipole rotator with an angular velocity Ω and magnetic moment vector μ , let its spin axis be along the z -axis, μ be in the (x, z) -plane, and α be the angle between Ω and μ . In polar coordinates,

$$\begin{aligned}\Omega &= \Omega(\cos \theta \hat{r} - \sin \theta \hat{\theta}), \\ \mu &= \mu[\cos(\theta - \alpha) \hat{r} - \sin(\theta - \alpha) \hat{\theta}].\end{aligned}\quad (2)$$

The corresponding magnetic field is

$$\mathbf{B}(\mathbf{r}) = \frac{\mu}{2r^3} [2 \cos(\theta - \alpha) \hat{r} + \sin(\theta - \alpha) \hat{\theta}], \quad (3)$$

where $\mu = B_p R^3/2$, B_p and R are the stellar radius and surface magnetic field at the pole, respectively (see, e.g., Zhang &

Harding 2000), and \hat{r} and $\hat{\theta}$ are the unit vectors of the radial and polar angle directions, respectively. For a pulsar with a period P and a period derivative \dot{P} , B_p is estimated by

$$B_p \approx 6.4 \times 10^{19} (P\dot{P})^{1/2} \text{ G}. \quad (4)$$

It is believed that the outer gap extends from its inner boundary to the light cylinder (CHR I). For an oblique magnetic dipole rotator, the polar angle θ_c for which the last open field line is tangent to the light cylinder is given by (Kapoor & Shukre 1998)

$$\tan \theta_c = -\frac{3}{4 \tan \alpha} \left[1 + (1 + 8 \tan^2 \alpha / 9)^{1/2} \right], \quad (5)$$

and the corresponding radius is

$$r_c = \frac{R_L}{\sin \theta_c}. \quad (6)$$

It should be noted that $\theta_c = \pi/2$ and $r_c = R_L$ for an aligned magnetic dipole. Along the last open field line, the relation

$$\frac{\sin^2(\theta - \alpha)}{r} = \frac{\sin^2(\theta_c - \alpha)}{r_c} \quad (7)$$

is valid. The inner boundary of the outer gap is estimated by the null-charge surface, which is defined by $\Omega \cdot \mathbf{B} = 0$. In the two-dimensional case, the null-charge surface can be described by $(r_{\text{in}}, \theta_{\text{in}})$. By definition, we have

$$\tan \theta_{\text{in}} = \frac{1}{2} \left(3 \tan \alpha + \sqrt{9 \tan^2 \alpha + 8} \right), \quad (8)$$

while r_{in} is estimated along the last open field line, which gives, using equation (7),

$$\frac{r_{\text{in}}}{R_L} = \frac{\sin^2(\theta_{\text{in}} - \alpha)}{\sin \theta_c \sin^2(\theta_c - \alpha)}. \quad (9)$$

Therefore, the outer gap extends from r_{in} to r_c along the last open field line for the oblique magnetic dipole. In such a geometry, the Goldreich-Julian current is roughly

$$\dot{N}_{\text{GJ}} \approx \frac{\Omega^2 R^3 B_p}{2ec} a(\alpha) \cos \alpha, \quad (10)$$

where $a(\alpha) = \sin \theta_c \sin^2(\theta_c - \alpha)$.

2.2. X-Ray Field in the Magnetosphere

The observed spectra of X-ray emission from some rotation-powered pulsars indicate that there are at least two kinds of X-ray spectra. One consists of soft X-rays, which can be fitted by a blackbody spectrum with a single temperature, combined with a hard X-ray spectrum with a power-law distribution. Another has only a thermal spectrum. It is believed that the nonthermal components are most likely of magnetospheric origin, while the origin of the thermal components is less clear, because there are several mechanisms for production of thermal emission in the soft X-ray bands. Observationally, the

bulk of the soft X-ray emission between ~ 0.1 and 1 keV is well fitted by a double blackbody at two different temperatures. The ratio of the area of the hotter component to that of the colder one is typically very small ($\sim a \text{ few} \times 10^{-5}$). The colder component has been explained as resulting from thermal cooling, while the hotter one most likely comes from bombardment by high-energy particles (Greiveldinger et al. 1996). It is expected that pulsars younger than $\sim 10^5$ yr will have significant neutron star cooling components. We briefly describe the main possible mechanisms of X-ray production below.

2.2.1. Thermal X-Ray Emission from Neutron Star Cooling

For thermal X-ray emission due to neutron star cooling, it is believed that its spectrum can be expressed with a modified blackbody; we approximate it as a blackbody spectrum with a temperature T_c . Because neutron star cooling concerns many different mechanisms, the estimate of the temperature T_c contains different uncertainties for different models. For example, the temperature can be expressed as (Romani 1996)

$$T_{c,6} \approx \left(\frac{\tau}{10^5 \text{ yr}} \right)^{-0.05} \exp\left(-\frac{\tau}{10^6 \text{ yr}}\right) \text{ K}, \quad (11)$$

where $T_{c,6}$ is the temperature of the neutron star cooling in units of 10^6 K and τ is the neutron star's age. The above expression is valid for τ less than several 10^6 yr. Zhang & Harding (2000) approximated the temperature T_c as

$$T_{c,6} = \begin{cases} 10^{-0.23} \tau_6^{-0.1}, & \tau \leq 10^{5.2} \text{ yr}, \\ 10^{-0.55} \tau_6^{-0.5}, & \tau > 10^{5.2} \text{ yr}, \end{cases} \quad (12)$$

where τ_6 is the age in units of 10^6 yr. Based on the cooling model derived from Tsuruta (1998) (in this model, the effects of the magnetic field on thermal conductivity are included, but polar-cap heating is not considered), Hirschman & Arons (2001) use a temperature model

$$T_{c,6}(t) = \begin{cases} 10^{0.05} \tau_6^{-0.1}, & \tau < 10^7 \text{ yr}, \\ 10^{0.325} \tau_6^{-0.375}, & \tau > 10^7 \text{ yr}, \end{cases} \quad (13)$$

where t is the spin-down age of the neutron star. For the hotter component originating from the bombardment by high-energy particles, the particles are produced in either the polar-cap region or the outer-gap region, resulting in different properties. In other words, the origin of the relativistic particles, which bombard the stellar surface to produce hotter thermal X-rays, depends on the models.

2.2.2. X-Ray Emission from Polar-Cap Heating

In the polar-cap models, the returning relativistic particles are produced in the polar gap (e.g., Ruderman & Sutherland 1975; Arons 1981). Recently, Zhang & Harding (2000) considered the full polar-cap cascade scenario of the polar-cap model and estimated the thermal X-ray luminosity using a self-consistent polar-cap heating in the Harding & Muslimov (1998) model (for a relevant recent study, see Hirschman & Arons 2001). Furthermore, Harding & Muslimov (2001) studied the effect of pulsar polar-cap heating produced by positrons returning from the upper pair formation front; the

polar-cap heating produces thermal X-ray emission with a temperature $T_{pc} = (L_{pc}/\sigma_{SB}A)^{1/4}$,

$$T_{pc,6} = \begin{cases} 2.46 \left(\frac{P_{0.1}}{\tau_6} \right)^{1/28} \left[\frac{\cos^2 \alpha}{a(\alpha)} \right]^{1/4}, & P_{0.1}^{9/4} < 0.5 B_{12}, \\ 2.51 P_{0.1}^{1/8} \left[\frac{\cos^2 \alpha}{a(\alpha)} \right]^{1/4}, & P_{0.1}^{9/4} > 0.5 B_{12}, \end{cases} \quad (14)$$

where L_{pc} is the X-ray luminosity emitted from the polar caps, σ_{SB} is the Stefan-Boltzmann constant, and A is the area heated by the positrons returning from the polar gaps. For the canonical polar-cap area, $A = A_{pc} = \pi R^2 (\Omega R/c)$. In the above expressions, $P_{0.1} = P/0.1$ s, $B_{12} = B/10^{12}$ G, and $\tau_6 = 10^6 \tau$ yr is the pulsar age. We have used the analytic estimate of X-ray luminosity given by Harding & Muslimov (2001) and A_{pc} , so the above expressions are valid for normal pulsars with $\tau \leq 10^7$ yr.

2.2.3. X-Ray Emission from Outer-Gap Heating

In the outer-gap models, some of the relativistic particles from the outer gap collide with the stellar surface, producing thermal X-rays. These relativistic inflowing particles from the outer gap radiate away much of their energy before reaching the polar cap (Zhang & Cheng 1997; Zhu & Ruderman 1997; Wang et al. 1998; Cheng & Zhang 1999). The residual energy of the charged particles striking the polar cap is

$$E_e(R) \approx \left(\frac{2e^2 c}{mc^3 R_L} \ln \frac{r}{R} \right)^{-1/3}. \quad (15)$$

These particles collide with the polar cap at a rate of $\dot{N}_e = f \dot{N}_{GJ}$, where \dot{N}_{GJ} is the Goldreich-Julian particle flux (Goldreich & Julian 1969) and is estimated by equation (10). Therefore, the polar cap is heated and radiates X-rays with a luminosity $[L_X \approx f E_e(R) \dot{N}_{GJ}]$

$$L_X \approx 2.3 \times 10^{31} f B_{12} P^{-5/3} \times R_6^3 \left(\ln \frac{r}{R} \right)^{-1/3} a(\alpha) \cos \alpha \text{ ergs s}^{-1}. \quad (16)$$

These X-rays have a typical temperature $T_h = (L_X/A\sigma_{SB})^{1/4}$ with

$$T_h \approx 5.0 \times 10^6 P^{-1/6} B_{12}^{1/4} \left(\ln \frac{r}{R} \right)^{-1/12} \times \sin^2[a(\alpha) \cos \alpha]^{1/4} \text{ K}, \quad (17)$$

where $A \sim \pi f \Omega R^3/c$ is the area of the stellar surface bombarded by the return current. Generally, some of these X-rays will escape along the open magnetic field lines. Following Cheng & Zhang (1999), we denote L_X^h as the luminosity of the X-rays escaping along the open field lines and introduce a parameter $\xi = L_X^h/L_X$ (the estimate of ξ ; see Cheng & Zhang 1999). Most of the X-rays are reflected back to the stellar surface through cyclotron resonance. This process transfers emitted polar-cap X-ray energy to the entire surface of the neutron star. Finally, the X-rays from the entire surface of the neutron star are emitted with a temperature $T = (L_X^s/2\pi R^2 \sigma_{SB})^{1/4}$, where

$L_X^s = (1 - \xi)L_X$. The corresponding characteristic temperature is $T_s = (L_X^s/4\pi R^2\sigma_{\text{SB}})^{1/4}$, which gives

$$T_s \approx 4.2 \times 10^5 (1 - \xi)^{1/4} f^{1/4} P^{-5/12} B_{12}^{1/4} \times \left(\ln \frac{r}{R}\right)^{-1/12} [a(\alpha) \cos \alpha]^{1/4} R_6^{1/4} \text{ K}. \quad (18)$$

2.2.4. Average Energy of the X-Rays

We consider two possible cases for the thermal X-rays from the stellar surface. In the first case, the thermal X-rays are produced by both the neutron star standard cooling mechanism and polar-cap heating. The temperatures are given by equation (12) or (13) for the standard cooling mechanism and equation (14) for the polar-cap heating. In the second case, the thermal X-rays come from the bombardment of relativistic particles from the outer gap (e.g., Zhang & Cheng 1997). The corresponding temperatures are given by equations (18) and (17). Assuming these X-rays can be approximated as black-body emission, their spectrum can be expressed as

$$F_X(E_X) = C \left(\frac{E_X^2}{e^{E_X/kT_1} - 1} + \frac{A}{4\pi R^2} \frac{E_X^2}{e^{E_X/kT_2} - 1} \right), \quad (19)$$

where R is the stellar radius, A is the area of the polar cap being heated, and T_1 and T_2 are the temperatures of the whole stellar surface and polar cap, respectively. Using the above expression, we can estimate the average X-ray energy as

$$\langle E_X \rangle = \frac{\int F_X(E_X) E_X dE_X}{\int F_X(E_X) dE_X} = \frac{\pi^4}{30\zeta(3)} \times \frac{1 + (A/4\pi R^2)(T_2/T_1)^4}{1 + (A/4\pi R^2)(T_2/T_1)^3} (kT_1), \quad (20)$$

where $\zeta(x)$ is the zeta function and $\zeta(3) \approx 1.2$. For the different mechanisms for thermal X-rays from the stellar surface, the dependence of $\langle E_X \rangle$ on the basic parameters of the pulsar is different.

We consider two possible ways to estimate the average X-ray energy.

1. If the thermal X-rays are produced by standard neutron star cooling and polar-cap heating, we have

$$\langle E_X^{\text{pc}} \rangle \approx 2.7kT_c \frac{1 + (R/4R_L)(T_{\text{pc}}/T_c)^4}{1 + (R/4R_L)(T_{\text{pc}}/T_c)^3}. \quad (21)$$

2. If the thermal X-rays are produced by the bombardment of relativistic particles from the outer gap, we have

$$\langle E_X^{\text{og}} \rangle \approx 2.7kT_s \frac{2 - \xi}{1 - \xi}. \quad (22)$$

2.3. The Fractional Size of the Outer Gap

In two-dimensional geometry, the fractional size of the outer gap is an important parameter for the γ -ray production there. According to Zhang & Cheng (1997), the parallel electric field in the outer gap can be approximated as

$$E_{\parallel} = f^2 B(r) (s/R_L), \quad (23)$$

where f is the fractional size of the outer gap,

$$B(r) = B_p [1 + 3 \cos^2(\theta - \alpha)]^{1/2} R^3/r^3$$

is the magnetic field strength at the radius r of the star, R_L is the radius of the light cylinder, and s is the curvature radius, which is (Lesch et al. 1998)

$$s(\theta, \theta_s) = \frac{R}{3} \frac{\sin(\theta - \alpha)}{\sin^2(\theta_s - \alpha)} \frac{[1 + 3 \cos^2(\theta - \alpha)]^{3/2}}{1 + \cos^2(\theta - \alpha)}, \quad (24)$$

where θ_s is the polar angle at the stellar surface. Equation (25) can be written as

$$s(\theta, \theta_s) = \sqrt{r R_L} W(\alpha, r), \quad (25)$$

with

$$W(\alpha, r) = \frac{4}{3} \frac{[1 - (3/4)a(\alpha)(r/R)]^{3/2}}{\sqrt{a(\alpha)}[1 - (1/2)a(\alpha)(r/R_L)]}, \quad (26)$$

where $a(\alpha) = \sin^2(\theta_c - \alpha) \sin \theta_c$. This electric field will accelerate the electrons and positrons to relativistic energy in the outer gap. Because these accelerated particles will lose their energy through curvature radiation, their Lorentz factor is estimated by using $eE_{\parallel}c = (2/3)e^2 c \gamma^4/s^2$, which gives

$$\gamma(r) \approx 2.84 \times 10^7 f^{1/2} B_{12}^{1/4} P^{-1/4} R_6^{3/4} \left(\frac{r}{R_L}\right)^{-3/8} \times \left[\frac{\sqrt{1 + 3 \cos^2(\theta - \alpha)}}{2} \right]^{1/4}, \quad (27)$$

where P is the pulsar period in units of seconds and R is the stellar radius in units of 10^6 cm. The characteristic energy of the γ -ray photons in the outer gap can be approximated as

$$E_{\gamma} \approx 143 f^{3/2} B_{12}^{3/4} P^{-7/4} \left[\frac{\sqrt{1 + 3 \cos^2(\theta - \alpha)}}{2} \right]^{3/4} \times \left(\frac{r}{R_L}\right)^{-3/2} \left(\frac{s}{R_L}\right)^{-1/4} R_6^{9/4} \text{ MeV}. \quad (28)$$

Inside the outer gap, the curvature photons interact with the thermal X-rays from the stellar surface to produce e^{\pm} pairs through a photon-photon pair-production process, sustaining the outer gap. This pair-production condition is

$$\langle E_X \rangle E_{\gamma} [1 - \cos(\theta_{X,\gamma})] = 2(m_e c^2)^2, \quad (29)$$

where $\langle E_X \rangle$ is the average X-ray energy, which is estimated below, and $\theta_{X,\gamma}$ is the angle between the emission directions of the curvature photons and the thermal X-rays. If we assume that the curvature photons are emitted along the negative direction of the magnetic field and the thermal X-rays along the radial direction, then we have

$$\cos \theta_{X,\gamma} = - \frac{2 \cos(\theta - \alpha)}{[3 \cos^2(\theta - \alpha) + 1]^{1/2}}, \quad (30)$$

where θ is the polar angle at radius r . Putting equation (7) into equation (30), we have

$$\cos \theta_{X,\gamma} = - \left[\frac{1 - (r/R_L)a(\alpha)}{1 - (3/4)(r/R_L)a(\alpha)} \right]^{1/2}, \quad (31)$$

where $a(\alpha) = \sin^2(\theta_c - \alpha) \sin \theta_c$.

We consider the fractional sizes of the outer gap corresponding to two possible average energies of the X-rays. In the first case, the X-rays are produced by neutron star cooling and polar-cap heating. The average X-ray energy is given by equation (21), and the fractional size of the outer gap is

$$f(r, \alpha) \approx 6.9 B_{12}^{-1/2} P^{7/6} \langle E_X \rangle_{0.1}^{-2/3} G_{pc}(r, \alpha), \quad (32)$$

with

$$G_{pc} = W^{1/6} \left(\frac{2}{1 - \cos \theta_{X,\gamma}} \right)^{2/3} \left(\frac{r}{R_L} \right)^{13/12} \times \left[\frac{\sqrt{1 + 3 \cos^2(\theta - \alpha)}}{2} \right]^{-1/2}, \quad (33)$$

where $\langle E_X \rangle_{0.1} = \langle E_X \rangle / 0.1$ keV. Because the temperature of the polar-cap heating is greater than that of the neutron star cooling, equation (21) can be approximated as $\langle E_X \rangle \approx 2.7 k T_c$. Using equations (12) and (13), respectively, we have

$$\langle E_X \rangle_{0.1} \approx \begin{cases} 32.9 \left(\frac{P}{\dot{P}} \right)^{-0.1}, & \dot{P}_{-15} \geq 10^2 P, \\ 5.2 \times 10^6 \left(\frac{P}{\dot{P}} \right)^{-0.5}, & \dot{P}_{-15} < 10^2 P, \end{cases} \quad (34)$$

$$\langle E_X \rangle_{0.1} \approx \begin{cases} 7.49 \left(\frac{P}{\dot{P}} \right)^{-0.11}, & \dot{P}_{-15} \geq 1.6 P, \\ 7.33 \times 10^4 \left(\frac{P}{\dot{P}} \right)^{-15/40}, & \dot{P}_{-15} < 1.6 P, \end{cases} \quad (35)$$

where $\dot{P} = 10^{-15} \dot{P}_{-15}$ is the period derivative of the pulsar in units of s^{-1} . In the second case, the thermal X-rays come from the bombardment of relativistic particles from the outer gap. Putting equations (28) and (20) into equation (29), we have

$$f(r, \alpha) \approx 5.2 B_{12}^{-4/7} P^{26/21} R_6^{10/7} G(r, \alpha), \quad (36)$$

with

$$G(r, \alpha) = \left(\frac{2}{1 - \cos \theta_{X,\gamma}} \right)^{4/7} \left(\ln \frac{r}{R} \right)^{1/21} \left(\frac{r}{R_L} \right)^{13/14} \times \left[\frac{W}{a(\alpha) \cos \alpha} \right]^{1/7} \left[\frac{\sqrt{1 + 3 \cos^2(\theta - \alpha)}}{2} \right]^{-3/7} \quad (37)$$

Obviously, f is a function of r , as well as the inclination angle α , in the two cases.

It is believed that the outer gap starts at the null-charge surface ($\Omega \cdot \mathbf{B} = 0$), which defines the inner boundary, and the radial distance is r_{in} . From equation (32) or (36), the fractional

size reaches a minimum at the radius (r_{in}) of the inner boundary and then increases with radius for a given pulsar. Therefore, the fractional size of the outer gap at the radius r_{in} determines whether or not the outer gap exists. If $f(r_{in}, \alpha) > 1$, it means that the pulsar does not have any outer gap. In other words, a pulsar with $f(r_{in}, \alpha) \leq 1$ should have an outer gap, which will emit high-energy photons. As the radius increases, the fractional size of the outer gap increases. For a pulsar with $f(r_c, \alpha) \leq 1$, the outer gap will extend from r_{in} to r_c . However, a pulsar with $f(r_c, \alpha) > 1$ will stop at some radius r_b at which $f(r_b, \alpha) = 1$. In order to explain the average properties of high-energy photon emission from the outer gap, we assume that high-energy emission at an average radius $\langle r \rangle$ represents the typical emission of high-energy photons from a pulsar. The average radius is given by

$$\langle r \rangle = \frac{\int_{r_{in}}^{r_{max}} f(r, \alpha) r dr}{\int_{r_{in}}^{r_{max}} f(r, \alpha) dr}, \quad (38)$$

where $r_{max} = \min(r_c, r_b)$. The average gap size is approximated as $f(\langle r \rangle, P, B)$ by substituting $\langle r \rangle$ into equations (32) and (36) and is in general a function of P, B , and α because r_c is a function of P and α , and r_b is a function of P, B , and α .

Generally, the inclination angles for the pulsars are not known well, so we consider the changes of fractional size with inclination angle. Let us define the function

$$f(\langle r \rangle, P, B) = \eta(\alpha, P, B) f_o(P, B), \quad (39)$$

where $f_o(P, B) = 5.5 P^{26/21} B_{12}^{-4/7}$ is the fractional size of the outer gap arrived at by ignoring the effect of the inclination angle (Zhang & Cheng 1997). Therefore, the effect of the inclination angle should be exhibited in the function $\eta(\alpha, P, B)$. In Figure 1 we consider the variation of outer-gap size with magnetic inclination angle for various P and B . In Figure 1a the upper and lower solid lines show the self-consistent outer-gap and the cooling X-ray outer-gap models, respectively, with $P = 0.1$ s, and the upper and lower dashed lines show the self-consistent outer-gap and the cooling X-ray outer-gap models, respectively, with $P = 0.3$ s. The magnetic field is chosen to be 3×10^{12} G. In Figure 1b the upper and lower solid lines show the self-consistent outer-gap and the cooling X-ray outer-gap models, respectively, with $B_{12} = 3.0$, and the upper and lower dashed lines show the self-consistent outer-gap and the cooling X-ray outer-gap models, respectively, with $B_{12} = 1.5$. The period is chosen to be 0.2 s. We can see that η varies by about a factor of 2 for the self-consistent model but becomes rather constant for the cooling X-ray outer-gap model.

3. HIGH-ENERGY γ -RAY LUMINOSITY

EGRET has observed six pulsars with high confidence and three possible radio pulsars emitting high-energy γ -rays above 100 MeV (see Thompson 2001 for a review). One of these possible radio pulsars is a millisecond pulsar, PSR J0218+4232 (Kuiper et al. 2000). Therefore, there could be eight young pulsars emitting high-energy γ -rays, based on observations by EGRET. It should be noted that PSR B1509-58 is also a γ -ray pulsar, but it is seen only up to 10 MeV by COMPTEL (Kuiper et al. 1999) and not above 100 MeV by EGRET. The observed γ -ray luminosity of a pulsar is $L_{\gamma}^{\text{obs}} = 4\pi d^2 \zeta F_{\gamma}$, where F_{γ} is the observed γ -ray flux, d is the distance to the pulsar, and ζ is the γ -ray beaming

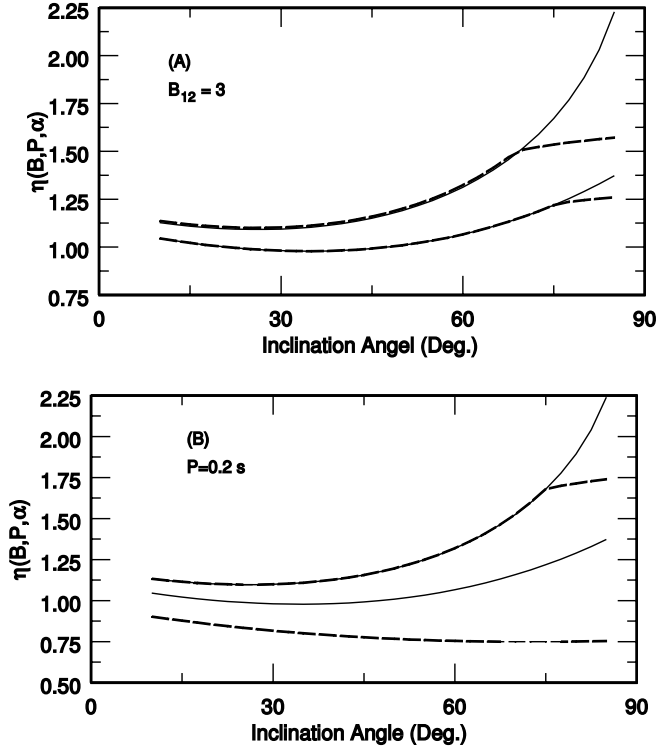


FIG. 1.—Variation of the fractional size of the outer gap with magnetic inclination angle for some typical pulsar parameters. (a) Plot of $\eta(P, B, \alpha)$ vs. α for a given magnetic field of 3×10^{12} G. The upper and lower solid lines show the self-consistent outer-gap and the cooling X-ray outer-gap models, respectively, with $P = 0.1$ s, and the upper and lower dashed lines show the self-consistent outer-gap and the cooling X-ray outer-gap models, respectively, with $P = 0.3$ s. (b) Plot of $\eta(P, B, \alpha)$ vs. α for a given period of 0.2 s. The upper and lower solid lines show the self-consistent outer-gap and the cooling X-ray outer-gap models, respectively, with $B_{12} = 3.0$, and the upper and lower dashed lines show the self-consistent outer-gap and the cooling X-ray outer-gap models, respectively, with $B_{12} = 1.5$.

fraction ($0 < \zeta \leq 1$), which is defined as the ratio of the beaming solid angle to 4π . Two parameters are highly uncertain: the distance d and the beaming fraction ζ . It is commonly assumed that $\zeta = 1/4\pi$ when estimating the observed γ -ray luminosity. However, the γ -ray beaming fraction should be different for various γ -ray pulsars, as a function of the magnetic inclination angle, as well as the size of the outer gap. Some approximations for the beaming fraction have been given (Yadigaroglu & Romani 1995; Romani 1996; Zhang, Zhang, & Cheng 2000). How accurate these approximations are is not known. Furthermore, we want to emphasize that, in addition to the beaming fraction, the distance estimate also affects the observed γ -ray luminosity strongly. For example, a recent measurement shows that the distance to the Vela pulsar is 294_{-50}^{+76} pc (Caraveo et al. 2001), which is less than the previous value (500 pc) derived from radio observation. Hence, the γ -ray luminosity of the Vela pulsar could be a factor of 2 lower than that given in Thompson (2001). In this paper we just want to see how the inclination affects the γ -ray luminosity. For simplification, we use the common assumption of $\zeta = 1/4\pi$ in order to compare with the observed data given by Thompson (2001).

Because high-energy γ -rays are mainly produced from the outer gap in our model, we compare our expected γ -ray luminosities with those of the γ -ray pulsars observed by EGRET. In our model, the γ -ray luminosity for each γ -ray pulsar depends on the period, magnetic field, and magnetic

inclination. However, the magnetic inclination angles are not known well. Once the average fractional size of the outer gap for a pulsar is estimated, the γ -ray luminosity can be approximated as

$$L_{\gamma} \approx f^3(\langle r \rangle) L_{sd}, \quad (40)$$

where $L_{sd} = 4\pi^2 I \dot{P} / P^3$ is the spin-down luminosity of the pulsar and $I = 10^{45}$ g cm². Using equation (4) and putting equation (36) into equation (40), we have

$$L_{\gamma} = L_{\gamma,0} \eta^3(\alpha, P, B), \quad (41)$$

with

$$L_{\gamma,0} \approx 1.36 \times 10^{33} B_{12}^{2/7} P^{-2/7}. \quad (42)$$

It is obvious that equation (42) is the same as that given by Zhang & Cheng (1997).

In principle, we can estimate the γ -ray luminosity for a pulsar with a known inclination angle. However, it is difficult to estimate the γ -ray luminosity for all canonical pulsars, because the inclination angles of only a few pulsars are known. Therefore, we find the statistical relation between γ -ray luminosity and pulsar spin-down power for canonical pulsars using a Monte Carlo method. The details of this Monte Carlo method are given by Cheng & Zhang (1998) and Zhang et al. (2000). We use the following assumptions to generate the Galactic pulsar population:

1. Pulsars are born at a rate $\dot{N}_{NS} \sim 1\text{--}2$ per century, with spin periods of $P_0 = 10$ ms.
2. The initial position for each pulsar is estimated from the distributions

$$\rho_z(z) = (1/z_{\text{exp}}) \exp(-|z|/z_{\text{exp}}),$$

$$\rho_R(R) = (a_R/R_{\text{exp}}^2) R \exp(-R/R_{\text{exp}}),$$

where z is the distance from the Galactic plane, R is the distance from the Galactic center, $z_{\text{exp}} = 75$ pc,

$$a_R = \left[1 - e^{-R_{\text{max}}/R_{\text{exp}}} (1 + R_{\text{max}}/R_{\text{exp}}) \right]^{-1},$$

$R_{\text{exp}} = 4.5$ kpc, and $R_{\text{max}} = 20$ kpc (Paczynski 1990; Sturmer & Dermer 1996).

3. The initial magnetic fields are distributed as a Gaussian in $\log B$, with a mean $\log B = 12.52$ and a dispersion $\sigma_B = 0.35$. We ignore any field decay for these rotation-powered pulsars.

4. The initial velocity of each pulsar is the vector sum of the circular rotation velocity at the birth location and a random velocity from the supernova explosion (Paczynski 1990; Cheng & Zhang 1998). The circular velocity is determined by the Galactic gravitational potential, and the random velocities are distributed as a Maxwellian with three-dimensional dispersion, $\sigma_v = \sqrt{3} \times 100$ km s⁻¹ (Lorimer, Bailes, & Harrison 1997).

5. A random distribution of magnetic inclination angles is used (e.g., Biggs 1990). However, the values of α are subject to two constraints. First, the photon energy given in equation (28) cannot be higher than the total potential drop of the outer gap. Second, r_{in} in equation (9) must be larger than the stellar radius.

The pulsar period at time t can be estimated by

$$P(t) = \left[P_0^2 + \left(\frac{16\pi^2 R_{\text{NS}}^6 B^2}{3Ic^3} \right) t \right]^{1/2}, \quad (43)$$

where R_{NS} is the neutron star radius and I is the neutron star moment of inertia. The period derivative (\dot{P}) can be determined by

$$P\dot{P} = (8\pi^2 R_{\text{NS}}^6 / 3Ic^3) B^2. \quad (44)$$

Furthermore, the pulsar position at time t is determined by following its motion in the Galactic gravitational potential. Using the equations given by Paczyński (1990) for a given initial velocity, the orbit integrations are performed using the fourth-order Runge-Kutta method with a variable time step (Press 1992) for the variables R , V_R , z , V_z , and ϕ . Then the sky position and the distance of the simulated pulsar can be calculated.

We now consider the observational selection effects. First, we consider radio selection effects in order to generate a pulsar population detectable at the radio band: the pulsar must have a radio flux greater than the radio survey flux threshold and a broadened pulse width less than the rotation period (e.g., Sturmer & Dermer 1996). The pulsar that satisfies

$$L_{400}/d^2 \geq S_{\text{min}} \quad (45)$$

is considered to be a radio-detectable pulsar, where L_{400} is the radio luminosity at 400 MHz and d is the distance to the pulsar. The radio beaming fraction can be expressed as (Emmering & Chevalier 1989)

$$f_r(\omega) = (1 - \cos \omega) + (\pi/2 - \omega) \sin \omega, \quad (46)$$

where $\omega = (6^\circ/2)P^{-1/2}$ (e.g., Biggs 1990) is the half-angle of the radio emission cone. Then, following Emmering & Chevalier (1989), a sample pulsar with a given period P is chosen in one out of $f_r(P)^{-1}$ cases using the Monte Carlo method. Second, we consider the γ -ray selection effects. According to Zhang et al. (2000), we use

$$S_\gamma(> 100 \text{ MeV}) \geq 1.2 \times 10^{-10} \text{ ergs cm}^{-2} \text{ s}^{-1} \quad (47)$$

as the minimum detectable γ -ray energy flux, which corresponds roughly to the faintest sources with $(TS)^{1/2} > 5$.

Using the above method, we can generate a γ -ray pulsar population. In Figure 2 we show the relation between γ -ray luminosity and spin-down power for the simulated γ -ray pulsar population using this new outer-gap model, in which the birth rate of the neutron stars is assumed to be 1 every 200 yr, and the pulsar ages are limited to be not greater than 10^7 yr. In this figure we show two pulsar populations, one for which radio selection effects of the pulsars with outer gaps are taken into account (i.e., radio-loud γ -ray pulsars; Fig. 2, filled circles), and the other, for radio-quiet γ -ray pulsars (Fig. 2, open circles).

There are several interesting features in this figure. First, there is a rather sharp boundary on the left of the population. In fact, this boundary is given by

$$L_\gamma = L_{\text{sd}}. \quad (48)$$

This relation/boundary results from the facts that γ -ray pulsars terminate at $f(\langle r \rangle) = 1$ and $r_{\text{max}} = r_b$ in equation (38).

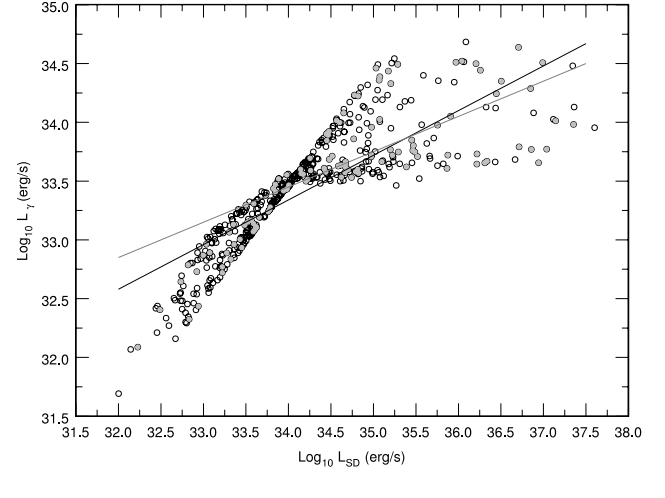


FIG. 2.—Change of γ -ray luminosity L_γ with the spin-down power L_{sd} in the γ -ray pulsar population predicted by our outer-gap model. In our simulation we have used the EGRET threshold as the minimum detectable γ -ray energy flux. Open and filled circles show the model radio-quiet and radio-loud γ -ray pulsars, respectively, and the solid line shows the best fit for all γ -ray pulsars with outer gaps. The lighter line is the best fit for the radio-loud γ -ray pulsars with outer gaps.

Similarly, the second rough boundary appearing at the bottom of the population is caused by $f(\langle r \rangle) = 1$ and $r_{\text{max}} = r_c = r_L$. Zhang & Cheng (1997) have estimated the fractional gap size by assuming that the typical distance from the gap to the star is $\sim r_L$; they obtained $f = 5.5B_{12}^{-4/7}P^{26/21}$. When we substitute this relation into L_{sd} , we obtain

$$L_{\text{sd}}^{\text{crit}} = 1.5 \times 10^{34} P^{1/3} \text{ ergs s}^{-1}. \quad (49)$$

It is important to note that $L_\gamma = L_{\text{sd}}$, as $L_{\text{sd}} \leq L_{\text{sd}}^{\text{crit}}$.

In such a pulsar population, the best fit gives the relation

$$\log L_\gamma \approx 20.42 + 0.38 \log L_{\text{sd}} \quad (50)$$

for the pulsars with outer gaps. When taking the radio selection effects into account, the L_γ - L_{sd} slope becomes flatter, i.e., $\log L_\gamma \approx 23.25 + 0.30 \log L_{\text{sd}}$. We consider the statistics of pulsars with outer gaps in the rest of this section. In order to show the important effect of the magnetic inclination angle on γ -ray luminosity, we show the change of $\log_{10}(L_\gamma/L_{\gamma,0})$ with $\log_{10} L_\gamma$ in Figure 3. The best fit indicates that $\log_{10}(L_\gamma/L_{\gamma,0}) \propto 0.9 \log_{10} L_\gamma$. For comparison, we show the result given by Zhang & Cheng (1997), which is independent of the inclination angle.

It is very interesting that the L_γ - L_{sd} slope becomes steeper when the minimum detectable γ -ray energy flux decreases. For example, obtaining a γ -ray pulsar population using the GLAST threshold ($1.8 \times 10^{-12} \text{ ergs cm}^{-2} \text{ s}^{-1}$), the best fit gives

$$\log L_\gamma \approx 17.45 + 0.46 \log L_{\text{sd}}. \quad (51)$$

That is, $L_\gamma \propto L_{\text{sd}}^{1/2}$. In this pulsar population, we have $\log_{10}(L_\gamma/L_{\gamma,0}) \propto 0.92 \log L_\gamma$.

For comparison, we show the results given by equations (50) and (51) and the observed high-energy photon luminosities of eight γ -ray pulsars in Figure 4. In this figure the observed data are taken from Thompson (2001), derived from detected fluxes above 1 eV assuming a solid angle of photon

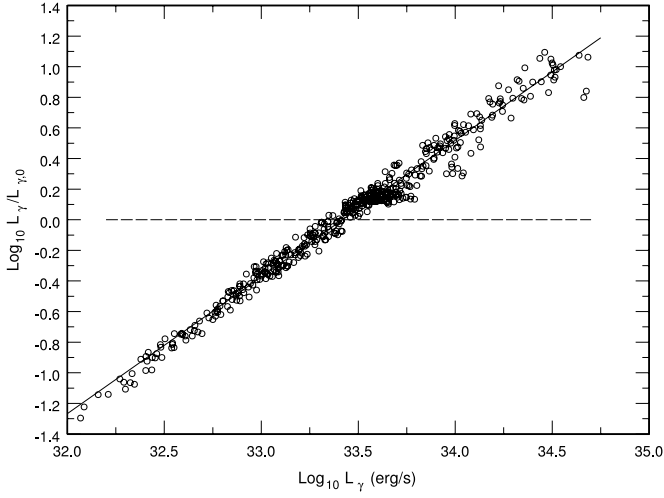


FIG. 3.—Plot of $L_\gamma/L_{\gamma,0}$ vs. L_γ in the γ -ray pulsar population predicted by our outer-gap model. In our simulation we have used the EGRET threshold as the minimum detectable γ -ray energy flux. Open circles show the expected data, and the solid line shows the best fit. For comparison, we show the result given by Zhang & Cheng (1997) as a dashed line.

beaming of 1 sr. From Figure 5 it can be seen that the results given by both equations (50) and (51) are consistent with the observed data. For the resulting fit of the simulated γ -ray pulsar population using the EGRET threshold, the expected slope (0.38) is flatter than the observed one (0.46).

Finally, we would like to point out that this new outer-gap model predicts many more weak γ -ray pulsars, whose γ -ray luminosities can be as low as 10^{32} ergs s^{-1} (e.g., Fig. 2), than previous outer-gap models (Zhang & Cheng 1997; Cheng & Zhang 1998). The main reason for these predicted weak γ -ray pulsars is that instead of using the outer-gap size at half the light cylinder radius to determine whether the outer gap can exist, the new model allows the outer gap to survive when the fractional size of the outer gap at the null-charge surface for a given pulsar is less than unity. This prediction allows the ages of γ -ray pulsars to extend to a few million years old. In fact, more detailed Monte Carlo simulation results show that most of these weak γ -ray pulsars have ages between 0.3 and 3 Myr,

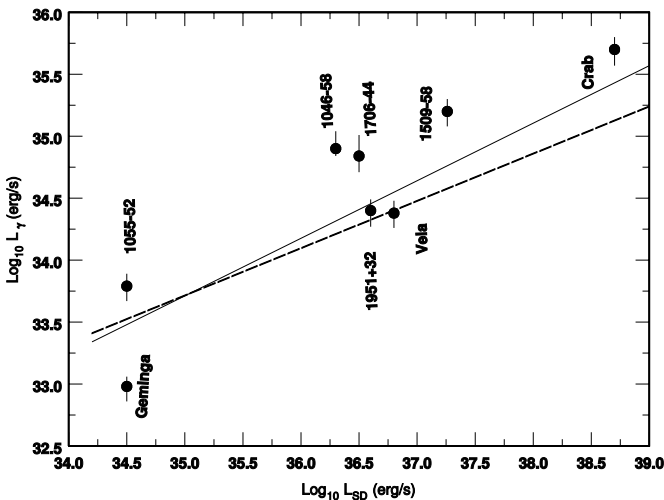


FIG. 4.— γ -ray luminosity vs. spin-down power. Filled circles with error bars show the data observed by Thompson (2001), and the solid and dashed lines show the results given by eqs. (50) and (51), respectively.

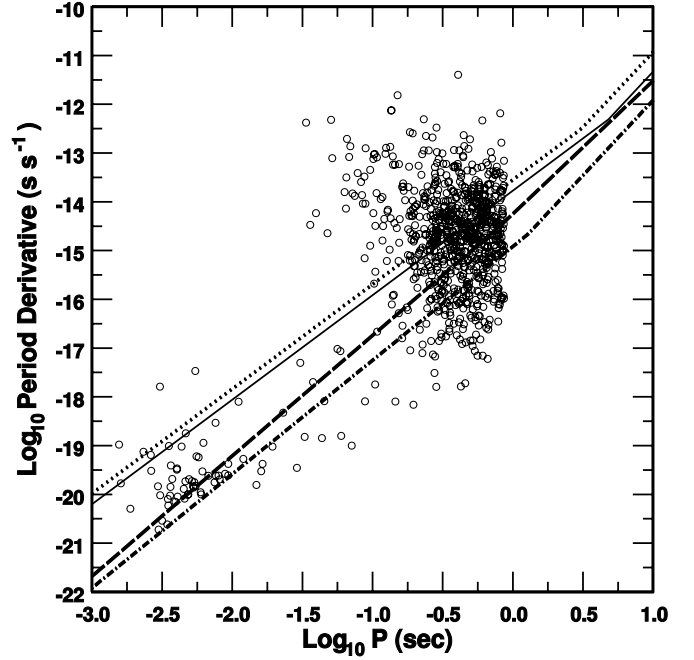


FIG. 5.—Death lines of pulsars with outer gaps. It is assumed that X-rays are produced by neutron star cooling and polar-cap heating. Two cases for the inclination angle distributions are considered: (1) a uniform distribution and (2) a cosine distribution. Dotted and solid lines show the death lines given by eqs. (56) and (59). Dashed and dot-dashed lines show the death lines given by eqs. (57) and (60). The observed data are taken from Web site <http://www.atnf.csiro.au/research/catalogue>.

and many of them are located at higher Galactic latitude. For most of these weak γ -ray pulsars, their radio beams could miss the Earth, and they would contribute to the unidentified γ -ray sources at high Galactic latitude (Cheng et al. 2003). These predictions can be verified by *GLAST*.

4. THE DEATH LINES OF PULSARS WITH OUTER GAPS

We now consider the condition for which the outer gap of a pulsar exists. For an outer gap, the inner boundary is estimated as the null-charge surface where the magnetic field lines are perpendicular to the rotation axis. From equation (36) or (32), $f(r, \alpha)$ reaches a minimum at $r = r_{in}$. In other words, if the fractional size of the outer gap at r_{in} were larger than unity, then the outer gap would not exist. Therefore, we can estimate the death lines of the pulsars with outer gaps by using $f(r_{in}, \alpha) = 1$. It should be noted that $G_{pc}(r_{in}, \alpha)$ in equation (32) and $G(r_{in}, \alpha)$ in equation (36) are functions only of α , because r_{in}/R_L depends only on α (see eq. [9]). For the case of X-rays produced by neutron star cooling and polar-cap heating, we obtain from $f(r_{in}, \alpha) = 1$

$$\log \dot{P} = \begin{cases} 3.1 \log P - A_1(\alpha), & \log P \leq 13 + \log \dot{P}, \\ \frac{15}{7} \log P - A_2(\alpha), & \log P > 13 + \log \dot{P}, \end{cases} \quad (52)$$

for the temperature given by Zhang & Harding (2000), where $A_1(\alpha) = 12.87 - 3.16 \log G_{pc}(\alpha)$ and $A_2(\alpha) = 12.92 - (12/7) \log G_{pc}(\alpha)$; and

$$\log \dot{P} = \begin{cases} 3.1 \log P - B_1(\alpha), & \log P \leq 14.8 + \log \dot{P}, \\ \frac{7}{3} \log P - B_2(\alpha), & \log P > 14.8 + \log \dot{P}, \end{cases} \quad (53)$$

for the temperature used by Hibschan & Arons (2001), where $B_1(\alpha) = 13.46 - 3.16 \log G_{pc}(\alpha)$ and $B_2(\alpha) = 13.95 - 2 \log G_{pc}(\alpha)$. For the case of X-rays produced by the bombardment of particles returning from the outer gap, we have

$$\log \dot{P} = \frac{10}{3} \log P - 13.02 + \frac{7}{2} \log G(\alpha). \quad (54)$$

Obviously, the death lines depend on the magnetic inclination angle.

Although the magnetic inclination angle of each pulsar has not been determined well, the distribution of the magnetic inclination angle can be estimated from a statistical polarization study of the radio pulsars. It was generally believed that the parent distribution of the magnetic inclinations is uniform (Gunn & Ostriker 1970; Gil & Han 1996). However, recent studies using the polarization data of radio pulsars indicate that the magnetic inclinations satisfy a cosine-like distribution (Tauris & Manchester 1998). Therefore, we estimate the average value of $f(r_{in}, \alpha)$ in these two possible parent distributions of the magnetic inclinations, i.e.,

$$\langle G(\alpha) \rangle = \frac{\int G(\alpha) U(\alpha) d\alpha}{\int U(\alpha) d\alpha}, \quad (55)$$

where $U(\alpha)$ represents the distribution of the inclination angles. We consider uniform and cosine-like distributions of the inclination angles separately. For the uniform distribution, we have $\langle G_{pc}(\alpha) \rangle \approx 0.32$ and $G(\alpha) = 0.38$. Therefore, equations (52), (53), and (54) become

$$\log \dot{P} = \begin{cases} 3.1 \log P - 14.43, & \log P \leq 13 + \log \dot{P}, \\ \frac{15}{7} \log P - 13.77, & \log P > 13 + \log \dot{P}, \end{cases} \quad (56)$$

$$\log \dot{P} = \begin{cases} 3.1 \log P - 15.02, & \log P \leq 14.8 + \log \dot{P}, \\ \frac{7}{3} \log P - 14.94, & \log P > 14.8 + \log \dot{P}, \end{cases} \quad (57)$$

$$\log \dot{P} = \frac{10}{3} \log P - 14.60. \quad (58)$$

For a cosine-like distribution, $\langle G_{pc}(\alpha) \rangle \approx 0.43$, $G(\alpha) \approx 0.49$, and equations (52), (53), and (54) become

$$\log \dot{P} = \begin{cases} 3.1 \log P - 14.03, & \log P \leq 13 + \log \dot{P}, \\ \frac{15}{7} \log P - 13.55, & \log P > 13 + \log \dot{P}, \end{cases} \quad (59)$$

$$\log \dot{P} = \begin{cases} 3.1 \log P - 14.62, & \log P \leq 14.8 + \log \dot{P}, \\ \frac{7}{3} \log P - 14.68, & \log P > 14.80 + \log \dot{P}, \end{cases} \quad (60)$$

$$\log \dot{P} = \frac{10}{3} \log P - 14.20. \quad (61)$$

Based on the original outer-gap model (CHR I; CHR II), Chen & Ruderman (1993) have considered the death lines of Crab-like and Vela-like pulsars. For Crab-like pulsars, the death line is (see eq. [25] of their paper)

$$\log \dot{P} = 4 \log P - 7. \quad (62)$$

For Vela-like pulsars, they introduced a parameter ξ to describe the expected variation of the magnetic field within the

outer gap and assumed $\xi = \frac{1}{2}$. In this case, the death line is (see eq. [27] of their paper)

$$\log \dot{P} = 3.8 \log P - 10.2. \quad (63)$$

According to Zhang & Cheng (1997), from

$$f_s \approx 2.83 \times 10^{-4} P^{20/21} \dot{P}^{-2/7} = 1,$$

we have

$$\log \dot{P} = \frac{10}{3} \log P - 12.42. \quad (64)$$

In Figure 5 we show the death lines of the pulsars with outer gaps for two possible distributions of the magnetic inclination angles. In this case we assume that X-rays are produced by neutron star cooling and polar-cap heating. Because the temperature used by Hibschan & Arons (2001) is higher than that used by Zhang & Harding (2000), the average energy of X-rays for the former work is greater than that for the latter. Therefore, the death lines obtained by using the temperature of Hibschan & Arons (2001) are lower than those from using the temperature of Zhang & Harding (2000).

In Figure 6 we show the death lines of pulsars with outer gaps, in which X-rays are produced by relativistic particles returning from the outer gap and the outer gap is self-sustained. For comparison, we also plot the death lines given by Chen & Ruderman (1993) and the death line derived from the model of Zhang & Cheng (1997). It can be seen that our model predicts that many more radio pulsars have self-sustained outer gaps compared to those given by Chen & Ruderman (1993), as well as by Zhang & Cheng (1997). In our estimate of the death lines

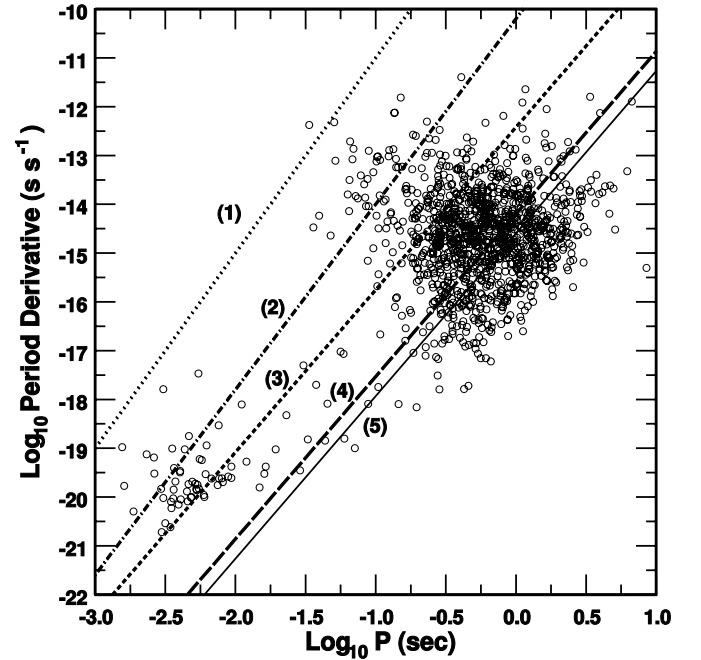


FIG. 6.—Death lines of pulsars with self-sustained outer gaps. The observed data are taken from Web site <http://www.atnf.csiro.au/research/catalogue>. Lines 1 and 2 are given by eqs. (62) and (63), respectively (Chen & Ruderman 1993). Line 3 is the death line (eq. [64]) predicted by Zhang & Cheng (1997). Lines 4 and 5 are the death lines of our model for the uniform and the cosine distributions of the inclination angles, respectively.

of pulsars with self-sustained outer gaps, we require that $f(r_{\text{in}}) = 1$. This condition is reasonable. It is believed that an outer gap can develop along the null-charge surface (Cheng et al. 1976) or along the last closed field line (CHR I; CHR II). Therefore, a self-sustained outer gap exists if the fractional size of the outer gap at r_{in} is not greater than unity.

5. DISCUSSION AND CONCLUSION

After taking into account the geometry of the dipole magnetic field, we have given a revised version of the outer-gap model given by Zhang & Cheng (1997). In the revised outer-gap model, the fractional size of the outer gap is the function not only of the period and magnetic field of the neutron star but also of the radial distance r to the neutron star and the magnetic inclination angle α . In other words, the fractional size of the outer gap has the form of $f(r, \alpha) = f_i(P, B_{12})G_i(r, \alpha)$, where $f_0(P, B_{12})$ is the function of only the pulsar period, and the surface magnetic field $G_i(r, \alpha)$ changes with radial distance to the neutron star and the magnetic inclination angle, where the subscript i represents the X-ray field considered. The fractional size of the outer gap is given by equation (32) in an X-ray field that is produced by neutron star cooling and polar-cap heating and by equation (36) in an X-ray field that is produced by outer-gap heating. In this model the fractional size of the outer gap has a minimum at the inner boundary for a given pulsar, increases with radial distance along the last open field lines, and then reaches its outer boundary, where $f(r_b, \alpha) = 1$. In other words, the outer gaps of some pulsars do not exist between the null-charge surface and the light cylinder. We have shown the changes of the fractional size of the outer gap with inclination angle (see Fig. 1). Furthermore, we have found that the outer gaps of relatively young pulsars, such as Vela, can extend from the null-charge surface to the light cylinder for any inclination angle; however, the outer gaps of some pulsars, such as Geminga, cannot extend to the light cylinder for a larger inclination angle (e.g., 75°).

In order to describe the average properties of high-energy radiation from a γ -ray pulsar, we have defined an average radial distance $\langle r \rangle$ (see eq. [38]). Using the Monte Carlo method described by Cheng & Zhang (1998) (see also Zhang et al. 2000), we simulated two populations of γ -ray pulsars, whose energy fluxes are greater than the EGRET threshold and *GLAST* threshold, respectively. In these simulations we considered only the population of pulsars with self-sustained outer gaps and a uniform distribution of inclination angles. We plotted the change of L_γ with L_{sd} (see Fig. 2). We also indicated the variation of $L_\gamma/L_{\gamma,0}$ with L_γ in Figure 3, which shows the importance of the inclination angle for L_γ . In the model of Zhang & Cheng (1997), L_γ is independent of the inclination angle. Fitting the simulated results, we found that $L_\gamma \propto L_{\text{sd}}^{0.38}$ for the EGRET threshold, and $L_\gamma \propto L_{\text{sd}}^{0.46}$ for the *GLAST* threshold. Compared with the observed data given by Thompson (2001), our simulated results are reasonable (see Fig. 4). In fact, the current distance of the Vela pulsar (Caraveo et al. 2001) is less than that used by Thompson (2001) by about a factor of 2, which reduces the luminosity by about a factor of 4.

In Figure 4 we note that Geminga is not within the simulated population. Zhang & Cheng (2001) have used a three-dimensional outer-gap model to explain the phase-resolved spectra of Geminga. They discovered that in order to fit the observed γ -ray data, the solid angle $\Delta\Omega$ must be near 5 sr. In Figure 4 $\Delta\Omega = 1$ sr is used for all observed γ -ray pulsars. If the larger solid angle is used, it brings Geminga

within the simulated population. It should be pointed out that Yadigaroglu & Romani (1995) have studied the effect of γ -ray beaming in their outer-gap model (see also Romani 1996). Zhang et al. (2000) also gave an approximate expression for the γ -ray beaming fraction, which will be applied to the estimated γ -ray fluxes in our new model.

It is interesting to point out that both polar-gap and outer-gap models predict $L_\gamma = L_{\text{sd}}$ for low spin-down power pulsars. But the position of the break occurs at $5 \times 10^{33} P^{-1/2}$ ergs s $^{-1}$ for the polar-gap model (Harding et al. 2002), whereas the outer-gap model predicts a higher position, at $1.5 \times 10^{34} P^{1/3}$ ergs s $^{-1}$. For higher spin-down power pulsars, the polar-gap model predicts $L_\gamma = L_{\text{sd}}^{1/2}$, whereas the outer-gap model cannot give a precise prediction, because the model L_γ also depends on the less well known parameter α . The statistical predictions of the outer-gap model give $L_\gamma = L_{\text{sd}}^\delta$, where δ depends on the properties of the γ -ray detector. For example, $\delta = 0.38$ for EGRET and 0.46 for *GLAST*.

According to our model, the fractional size of the outer gap at the null-charge surface for a given pulsar [$f(r_{\text{in}}, \alpha)$] reaches a minimum. Therefore, the outer gap should exist only if $f(r_{\text{in}}, \alpha) \leq 1$. Averaging $f(r_{\text{in}}, \alpha)$ for two possible distributions (uniform and cosine) of the magnetic inclination angle, we obtained the death lines of pulsars with outer gaps in the two possible X-ray fields and compared them with the observed data in Figures 5 and 6. Compared to the death line derived from the outer-gap model of Zhang & Cheng (1997), the revised model predicts that more pulsars will have outer gaps and then emit high-energy photons.

We make the following conclusions: Our results indicate that (1) the intrinsic parameters for explaining the observed γ -ray properties of rotation-powered pulsars are the magnetic inclination angle, period, and magnetic field. We have obtained a very concrete functional form for the prediction of γ -ray luminosity that depends only on these intrinsic parameters; the inclination angle could be known if the radio data were sufficiently good. (2) The conversion efficiencies for seven known γ -ray pulsars, which have rather scattered values, can be explained in our revised model using the Monte Carlo method. Although our estimation of the outer-gap size cannot be precise for an individual pulsar when the magnetic inclination angle is poorly known, it is a reasonable estimation of the statistical properties of γ -ray pulsars using the statistical method. (3) Unlike those seven observed γ -ray pulsars, mature pulsars (ages 0.3–3 Myr) can also be γ -ray pulsars, and their efficiency is insensitive to the inclination angle. Most importantly, their γ -ray luminosity is proportional to the spin-down power, which can be tested by *GLAST*. (4) The mean cutoff age of γ -ray pulsars is increased by a factor of 3; therefore, older γ -ray pulsars (up to about 3 Myr old) can move up to a higher Galactic latitude. Some unidentified EGRET γ -ray sources could be the mature pulsars predicted by this model, with ages between 0.3 and 3 Myr. In fact, a Parkes Observatory survey has discovered a large number of radio pulsars on the error boxes of EGRET unidentified γ -ray point sources (Torres & Nuza 2003). (5) The previous works on death lines based on the outer-gap model (e.g., Chen & Ruderman 1993) did not give detailed physical motivations; rather, they used a phenomenological approach. Here we proposed a new criterion based on a concrete physical property regarding the death line, which predicts more γ -ray pulsars. (6) Our model predicts many more weak γ -ray pulsars, with ages between 0.3 and 3 Myr, than previous outer-gap models, and they satisfy $L_\gamma \propto L_{\text{sd}}$, which can be verified by *GLAST*.

Finally, we would like to remark that the γ -ray luminosity formulae developed in this paper may not be able to explain the γ -ray luminosity of an individual pulsar. Two important factors, i.e., distance uncertainty and beaming fraction, which play crucial roles in determining the γ -ray luminosity, have not been considered here. For example, the luminosity ratio between PSR B1055–52 and Geminga, which have the same spin-down power of 3×10^{34} ergs s⁻¹, is about a factor of 6 (Thompson 2001), but the model ratio prediction (e.g., Fig. 2) is no more than a factor of 3. In fact, the estimate of the distance of PSR B1055–52 is very uncertain; it ranges from ~ 1.5 kpc (e.g., Thompson 2001) to a small value of ~ 500 pc (see, e.g., Ögelman & Finley 1993; Combi, Romero, & Azcarate 1997; Torres, Butt, & Camilo 2001; Hirotani & Shibata 2002), which makes the ratio change from ~ 10 to ~ 3 . A recent distance estimate for PSR B1055–52 from the dispersion measure is ~ 0.72 kpc (see Mignani, De Luca, & Caraveo 2003).⁴ However, it is well known that a 25% error is

common in determining the dispersion measure (McLaughlin & Cordes 2000), which gives a factor of 2 uncertainty in the luminosity. In addition, the distance estimate of Geminga is known to have at least a 25% uncertainty (Caraveo et al. 1996), which gives another factor of 2 uncertainty in the γ -ray luminosity estimate. Other uncertainty results from the γ -ray beaming fraction. In principle, obtained values for both the distance estimate and beaming fraction will be more accurate in the future. Our model still predicts that the difference in the magnetic inclination angle can cause a large difference in γ -ray luminosity for pulsars with the same spin-down power.

We thank the anonymous referee for his/her very constructive comments. This work is partially supported by the Hundred Talents Program of the Chinese Academy of Sciences, National 973 Key Project of China (NKBRSCF 19990754), and an RGC grant of the Hong Kong government.

⁴ See http://rsd-www.nrl.navy.mil/7213/lazio/ne_model.

REFERENCES

- Arons, J. 1981, *ApJ*, 248, 1099
 Biggs, J. D. 1990, *MNRAS*, 245, 514
 Caraveo, P. A., Bignami, G. F., Mignani, R., & Taff, L. G. 1996, *ApJ*, 461, L91
 Caraveo, P. A., De Luca, A., Mignani, R. P., & Bignami, G. F. 2001, *ApJ*, 561, 930
 Chen, K., & Ruderman, M. A. 1993, *ApJ*, 402, 264
 Cheng, A. F., Ruderman, M. A., & Sutherland, P. G. 1976, *ApJ*, 203, 209
 Cheng, K. S., Ho, C., & Ruderman, M. A. 1986a, *ApJ*, 300, 500 (CHR I)
 ———. 1986b, *ApJ*, 300, 522 (CHR II)
 Cheng, K. S., & Zhang, L. 1998, *ApJ*, 498, 327
 ———. 1999, *ApJ*, 515, 337
 Cheng, K. S., et al. 2003, *ApJ*, submitted
 Combi, J. A., Romero, G. E., & Azcarate, I. N. 1997, *Ap&SS*, 250, 1
 Daugherty, J. K., & Harding, A. K. 1996, *ApJ*, 458, 278
 Dermer, C. D., & Sturmer, S. J. 1994, *ApJ*, 420, L75
 Emmering, R. T., & Chevalier, R. A. 1989, *ApJ*, 345, 931
 Gil, J. A., & Han, J. L. 1996, *ApJ*, 458, 265
 Goldreich, P., & Julian, W. H. 1969, *ApJ*, 157, 869
 Greiveldinger, C., et al. 1996, *ApJ*, 465, L35
 Gunn, J. E., & Ostriker, J. P. 1970, *ApJ*, 160, 979
 Harding, A. K. 1981, *ApJ*, 245, 267
 Harding, A. K., & Muslimov, A. G. 1998, *ApJ*, 508, 328
 ———. 2001, *ApJ*, 556, 987
 Harding, A. K., Muslimov, A. G., & Zhang, B. 2002, *ApJ*, 576, 366
 Hibsman, J. A., & Arons, J. 2001, *ApJ*, 554, 624
 Hirotani, K. 2001, *ApJ*, 549, 495
 Hirotani, K., Harding, A. K., & Shibata, S. 2003, *ApJ*, 591, 334
 Hirotani, K., & Shibata, S. 2001, *ApJ*, 558, 216
 ———. 2002, *ApJ*, 564, 369
 Holloway, N. J. 1973, *Nature Phys. Sci.*, 246, 6
 Kapoor, R. C., & Shukre, C. S. 1998, *ApJ*, 501, 228
 Kaspi, V. M., Lackey, J., Mattox, J., Manchester, R. N., & Bailes, M. 2000, *ApJ*, 528, 445
 Kuiper, L., Hermsen, W., Krijger, J. M., Bennett, K., Carramiñana, A., Schönfelder, V., Bailes, M., & Manchester, R. N. 1999, *A&A*, 351, 119
 Kuiper, L., Hermsen, W., Verbunt, F., Thompson, D. J., Stairs, I. H., Lyne, A. G., Strickman, M. S., & Cusumano, G. 2000, *A&A*, 359, 615
 Lesch, H., Jessner, A., Kramer, M., & Kunzl, T. 1998, *A&A*, 332, L21
 Lorimer, D. R., Bailes, M., & Harrison, P. A. 1997, *MNRAS*, 289, 592
 McLaughlin, M. A., & Cordes, J. M. 2000, *ApJ*, 538, 818
 Mignani, R. P., De Luca, A., & Caraveo, P. A. 2003, in *IAU Symp. 218, Young Neutron Stars and Their Environments*, ed. F. Camilo & B. M. Gaensler (San Francisco: ASP), in press (astro-ph/0311468)
 Ögelman, H., & Finley, J. P. 1993, *ApJ*, 413, L31
 Paczyński, B. 1990, *ApJ*, 348, 485
 Press, W. H. 1992, *Numerical Recipes in C: The Art of Scientific Computing* (2nd ed.; Cambridge: Cambridge Univ. Press)
 Romani, R. W. 1996, *ApJ*, 470, 469
 Romani, R. W., & Yadigaroglu, I. A. 1995, *ApJ*, 438, 314
 Rudak, B., & Dyks, J. 1998, *MNRAS*, 295, 337
 Ruderman, M. A., & Sutherland, P. G. 1975, *ApJ*, 196, 51
 Sturmer, S. J., & Dermer, C. D. 1996, *ApJ*, 461, 872
 Tauris, T. M., & Manchester, R. N. 1998, *MNRAS*, 298, 625
 Thompson, D. J. 2001, in *AIP Conf. Proc. 558, High Energy Gamma-Ray Astronomy*, ed. F. A. Aharonian & H. J. Volk (New York: AIP), 103
 Torres, D. F., Butt, Y. M., & Camilo, F. 2001, *ApJ*, 560, L155
 Torres, D. F., & Nuza, S. E. 2003, *ApJ*, 583, L25
 Tsuruta, S. 1998, *Phys. Rep.*, 292, 1
 Wang, F. Y.-H., Ruderman, M., Halpern, J. P., & Zhu, T. 1998, *ApJ*, 498, 373
 Yadigaroglu, I.-A., & Romani, R. W. 1995, *ApJ*, 449, 211
 Zhang, B., & Harding, A. K. 2000, *ApJ*, 532, 1150
 Zhang, L., & Cheng, K. S. 1997, *ApJ*, 487, 370
 ———. 1998, *MNRAS*, 294, 177
 ———. 2001, *MNRAS*, 320, 477
 Zhang, L., Zhang, Y. J., & Cheng, K. S. 2000, *A&A*, 357, 957
 Zhu, T., & Ruderman, M. 1997, *ApJ*, 478, 701